Molecular and Cellular Neuroscience 75 (2016) 50–62

Contents lists available at ScienceDirect

Molecular and Cellular Neuroscience

journal homepage: www.elsevier.com/locate/ymcne

An electrophysiological study on the effects of BDNF and FGF2 on voltage dependent Ca^{2+} currents in developing human striatal primordium

Roberta Squecco [a,*], Eglantina Idrizaj [a], Annamaria Morelli [b], Pasquale Gallina [c], Gabriella B. Vannelli [b], Fabio Francini [a]

[a] Department of Experimental and Clinical Medicine, Section of Physiological Sciences, University of Florence, viale Morgagni 63, 50134 Florence, Italy
[b] Department of Experimental and Clinical Medicine, Section of Anatomy and Histology, University of Florence, Largo Brambilla 3, 50134 Florence, Italy
[c] Department of Surgery and Translational Medicine, University of Florence, Largo Palagi 1, 50139 Florence, Italy

ARTICLE INFO

Article history:
Received 31 January 2016
Revised 24 May 2016
Accepted 27 June 2016
Available online 28 June 2016

Keywords:
Human striatal primordium
Neurotrophic factor BDNF
Neurotrophic factor FGF2
Electrophysiology

ABSTRACT

Over the past decades, studies in both Huntington's disease animal models and pilot clinical trials have demonstrated that replacement of degenerated striatum and repair of circuitries by grafting fetal striatal primordium is feasible, safe and may counteract disease progression. However, a better comprehension of striatal ontogenesis is required to assess the fetal graft regenerative potential. During neuronal development, neurotrophins exert pleiotropic actions in regulating cell fate and synaptic plasticity. In this regard, brain-derived neurotrophic factor (BDNF) and fibroblast growth factor 2 (FGF2) are crucially implicated in the control of fate choice of striatal progenitor cells. In this study, we intended to refine the functional features of human striatal precursor (HSP) cells isolated from ganglionic eminence of 9–12 week old human fetuses, by studying with electrophysiological methods the effect of BDNF and FGF2 on the membrane biophysical properties and the voltage-dependent Ca^{2+} currents. These features are particularly relevant to evaluate neuronal cell functioning and can be considered reliable markers of the developmental phenotype of human striatal primordium. Our results have demonstrated that BDNF and FGF2 induced membrane hyperpolarization, increased the membrane capacitance and reduced the resting total and specific conductance values, suggesting a more efficient control of resting ionic fluxes. Moreover, the treatment with both neurotrophins enhanced N-type Ca^{2+} current amplitude and reduced L- and T-type ones. Overall, our data indicate that BDNF and FGF2 may help HSP cells to attain a more functionally mature phenotype.

1. Introduction

In the human brain, the corpus striatum is composed of two large subcortical nuclear masses, the caudate nucleus and the putamen, similar in their constituent neurons, intrinsic circuits, and neurophysiology. These nuclei are the main part of the basal ganglia and work with the cortex through a complex network to co-ordinate movements, cognition and emotion, thus controlling the execution of planned and motivated behaviors (Obeso et al., 2008). Selective neuronal loss of the striatum, accounts for most of the clinical features of Huntington's disease (HD), a genetic neurodegenerative disorder characterized by cognitive, motor and psychiatric impairments, which inexorably leads to death within 15–30 years (Novak and Tabrizi, 2010). No proven medical treatments are currently available to counteract the devastating course of the disease. Over the past decades, studies in both HD animal models (Peschanski et al., 1995; Armstrong et al., 2000) and pilot clinical trials (Bachoud-Lévi et al., 2006; Reuter et al., 2008; Gallina et al., 2010; Zuccato et al., 2010; Onorati et al., 2014; Paganini et al., 2014) have demonstrated that replacement of degenerated striatum and repair of circuitries by grafting fetal striatal primordium is feasible, safe and may counteract disease progression, thus prospecting an effective strategy to treat HD patients. The achievement of this practice depends on the ability of the grafted cells to proliferate, differentiate, and re-establish impaired circuitries (Tuszynski, 2007). However, several causes may hamper graft survival, such as hypoxia, mechanical

Abbreviations: BDNF, brain-derived neurotrophic factor; C_m, cell capacitance; FGF2, fibroblast growth factor 2; G_m, resting membrane conductance; G_m/C_m, specific conductance; G_{max}, maximal conductance for the activating current; HD, Huntington's disease; HP, holding potential; HSP, human striatal precursor; HVA, high voltage-activated Ca^{2+} currents; I_a, activating current; I_{Ca}, Ca^{2+} currents; $I_{Ca,max}/C_m$, current specific maximal size; I_m, steady-state membrane current; k_a, steepness factor for activation curve; k_h, steepness factor for inactivation curve; LVA, low voltage-activated Ca^{2+} currents; R_a, access resistance; R_m, membrane resistance; RMP, resting membrane potential; τ, time constant of the transient's decay; V_a, potential eliciting the half-maximal activation; V_h, potential eliciting the half-maximal inactivation; V_{rev}, apparent reversal potential.

* Corresponding author.
E-mail address: roberta.squecco@unifi.it (R. Squecco).

http://dx.doi.org/10.1016/j.mcn.2016.06.008
1044-7431/

injury, neurotrophic factors deficiency and free radical production (Cicchetti et al., 2009; Watmuff et al., 2012). *In vitro* modelling is thus necessary to help understand how primordium cells could face those acute and chronic stressors, but several challenges remain to be faced before using this therapy widely. Hopefully, optimization of transplantation protocols and improvement of functional outcome may be reached thanks to a better comprehension of striatal ontogenesis and fetal tissue potential.

During neuronal development, neurotrophic factors exert pleiotropic actions in regulating cell fate, synaptic plasticity, as well as circuitry formation and maintenance (Park and Poo, 2013). In this regard, brain-derived neurotrophic factor (BDNF) and fibroblast growth factor 2 (FGF2) have been crucially implicated in the control of proliferation and fate choice of striatal progenitor cells (Grothe and Timmer, 2007; Cohen-Cory et al., 2010). In previous studies, we demonstrated that human striatal precursor (HSP) cells isolated from 9 to 12-week-old human fetuses, possessed the machinery for long-term survival, proliferation and differentiation (Sarchielli et al., 2014), even under hypoxic conditions (Ambrosini et al., 2015). In addition, this HSP cell plasticity was maintained *in vitro* by the mentioned neurotrophins BDNF and FGF2 in a peculiar manner. Indeed, if on one hand these neurotrophins promoted an undifferentiated state of HSP cells inducing neurogenesis, migration and survival, on the other hand, they stimulated neuritogenesis and thereby maturation of the main component of HSP cell population (Sarchielli et al., 2014). Since HSP cells endogenously produce BDNF and FGF2, these neurotrophins could also play an important autocrine–paracrine role in determining progenitor cell biology during early striatum development. Based on this background (for a review see Zuccato et al., 2010) and on recently published research (Onorati et al., 2014), we here intended to focus the present electrophysiological study on the effect of BDNF and FGF2 treatment on the passive membrane properties and the different voltage-dependent Ca^{2+} currents present in neuronal cells from HSP, known to be good marker of the cell fate. In fact, the expression of the type of Ca^{2+} channels depends on the stage of differentiation, on the type of neuron considered and of transcripts expressed. Ca^{2+} currents are usually small or absent in mesenchymal (Benvenuti et al., 2006; Heubach et al., 2004; Li et al., 2005) or neuronal stem cell (Moe et al., 2005) but appear in neuronal precursors with a prevalent L-type current (D'Ascenzo, et al., 2006). Therefore, the early appearance of L-type Ca^{2+} current has a privileged role in the regulation of gene transcription. In contrast, N-, P/Q- and R-type Ca^{2+} channels are expressed later and are primarily responsible for initiation of synaptic transmission early in development and during maturation in most systems studied to date (Reid et al., 2003; Catterall and Swanson, 2015). Of note, the sensitivity to growth factors varies among the different types of Ca^{2+} currents and the different kinds of neurons: in fact, a specific growth factor can determine opposite effects such as enhancement or inhibition with different strength, time-dependence and may dramatically differ depending on how it is delivered (Ji et al., 2010). Based on this background and on recently published research (Onorati et al., 2014), we here intended to focus the present electrophysiological study on the effect of BDNF and FGF2 treatment on the passive membrane properties and the different voltage-dependent Ca^{2+} currents present in neuronal cells from HSP (n-HSP). To date, in fact, the effects of these growth factors on the electrical properties of the newly formed fetal human striatal precursors have been scarcely investigated. Actually, whether neuronal progenitor cells exhibit voltage- and ligand-gated currents, features characteristic of neurons, and whether these currents are differentially regulated by growth conditions is an important question that has already been addressed in previous studies in different cell models (Sah et al., 1997). Consequently, the present results are particularly relevant to show that neurotrophins treatment of human striatal precursors significantly enhances the acquisition of functional features, indicative of a mature neuronal phenotype.

2. Materials and methods

2.1. Cell cultures

The primary human striatal precursor (HSP) cells were isolated and propagated *in vitro* from human fetal striatal primordium of 9–12 week-old legally aborted fetuses, as described previously (Gallina et al., 2008, 2010; Sarchielli et al., 2014). The use of human fetal tissue for research purposes was approved by the National Ethics Committee and the Committee for investigation in Humans of the University of Florence (Protocol no 678304). HSP cells are a mixed population including neural stem cells, glial- and neuronal-committed progenitors and mature neurons with a striatal phenotype, with this latter component being highly expressed, as previously demonstrated by an extensive characterization (Sarchielli et al., 2014; Ambrosini et al., 2015). For electrophysiological experiments, 10^5 cells were seeded onto coverslips, serum starved for 24 h and then stimulated with 50 ng/ml BDNF or 50 ng/ml FGF2 alone or after 30 min of preincubation with 200 nM of their receptor inhibitors k252a and PD173074, respectively. After a 24 h incubation (37 °C), the stimulated or unstimulated cells were analyzed by electrophysiology. In a further set of experiments, we tested the effects of both growth factors given in combination for 24 h (50 ng/ml FGF2 + 50 ng/ml BDNF). Finally, to test a time-dependence of the response to growth factors, we performed electrophysiological records under acute treatment and at a later time point (48 h).

All the electrophysiological recordings were performed in selected cells with a marked spindle-shaped neuronal morphology (n-HSP). The statistical analysis included only selected n-HSP showing: 1) voltage-dependent L-type Ca^{2+} currents and a RMP more negative than −40 mV, since cells that did not show L-type Ca^{2+} currents and with RMP more positive to such a value are usually considered stem cells (Heubach et al., 2004; Li et al., 2005; Moe et al., 2005; Benvenuti et al., 2006; D'Ascenzo et al., 2006); 2) a membrane time constant >10 ms, since glial-like cells, although have generally a RMP close to −70 mV, have a time constant definitely <10 ms (Westerlund et al., 2003) suggesting a less wide cell surface. Accordingly, the reported data are related to the cells that satisfied these criteria, namely the 70% of the patched control cells, the 84% of BDNF- and 82% of FGF2-treated cells.

2.2. Solutions for electrophysiological experiments

Coverslips with the adherent n-HSP cells in control medium were first superfused at a rate of 1.8 ml min^{-1} with a physiological bath solution having the following composition (mM): 150 NaCl, 5 KCl, 2.5 $CaCl_2$, 1 $MgCl_2$, 10 D-glucose and 10 HEPES (pH 7.4 with NaOH). To block the high voltage activated Na^+ channels sensitivity, we used TTX (1 μM). Ca^{2+} currents were recorded in a Na^+- and K^+-free solution, namely a TEA-Ca^{2+} bath solution, containing (mM): 10 $CaCl_2$, 145 TEABr and 10 HEPES. For the specific blockade of L-type Ca^{2+} channels, Nifedipine (Sigma) was diluted at 10^{-2} M in DMSO and stored at 4 °C; it was used at 3 μM. ω-Conotoxin-GVIA (ω-CTx-GVIA) and ω-agatoxin-IVA (ω-Aga-IVA (both from Alomone Labs, Jerusalem, Israel) were diluted in distilled water at 5×10^{-4} and 10^{-4} M, respectively, and stored at 20 °C; ω-CgTx-GVIA was used at 500 nM to specifically block N-type channels and ω-Aga-IVA at 200 nM to block P and Q-type channels. Drugs were prepared daily from stock solutions, just before use. To prevent degradation during the experiments nifedipine was stored in the dark and toxins at 4 °C. T-type currents were minimized by using a holding potential (HP) of −40 mV or by using Ni^{2+} (200 μM); thus, T-current was evaluated by subtracting the resulting current from the total Ca^{2+} currents. The recording pipettes were filled with a filling pipette solution containing (mM): 150 CsBr, 5 $MgCl_2$, 10 EGTA and 10 HEPES (pH 7.2 with KOH). To test the effects of dopaminergic agonists, SKF82958 (10 μM; Sigma-Aldrich) or quinpirole (10 μM, Sigma-

Aldrich), selective for D1- and D2-dopamine receptors, respectively, were acutely added to the bath solutions.

2.3. Electrophysiological stimulations and records

Low-resistance patch pipettes (3–7 MΩ) made from borosilicate glass tubing (Harvard apparatus LTD) using a vertical puller (Narishige, Tokyo, Japan) were used for whole-cell patch clamp recordings in voltage- or current-clamp condition. The whole-cell configuration was obtained after gentle application of negative pressure. Access resistance was continuously monitored during the experiments. Only those cells in which access resistance was stable (changes <10%) were analyzed. Pclamp6 (Axon Instruments, Foster City, CA) software was used for analysis. The technique, set up and electronics are as described in details in an earlier report (Benvenuti et al., 2006). Briefly, the patch pipette was connected to a micromanipulator and an Axopatch 200B amplifier (Axon Instruments). Voltage-clamp protocol generation and data acquisition were controlled by using an output and an input of the A/D-D/A interfaces (Digidata 1200; Axon Instruments) and Pclamp 9 software (Axon Instruments). Currents were low-pass filtered with a Bessel filter at 2 kHz. The stimulation protocol for activation was applied to the cell held at HP of −80 mV. 1-Second long test pulses ranged from −80 to 50 mV and were applied in 10 mV steps. The stimulation protocol for inactivation consisted of a voltage test step to −20 mV, preceded (prepulsed) by the same voltage pulses used for activation. The acquisition rate for activation was 10 kHz and 5 kHz for inactivation. The interpulse interval was 500 ms. Capacitive and leak currents were automatically subtracted from the records by the P4 procedure.

The steady-state ionic current activation was evaluated by

$$I_a(V) = G_{max}\,(V - V_{rev})/\{1 + \exp[(V_a - V)/k_a]\} \quad (1)$$

and steady-state inactivation by

$$I_h(V) = I/\{1 + \exp[-(V_h - V)/k_h]\}, \quad (2)$$

where G_{max} is the maximal conductance for the I_a, V_{rev} is the apparent reversal potential, V_a and V_h are the potentials eliciting the half-maximal size, k_a and k_h are the steepness factors.

Electrode capacitance was compensated before disrupting the patch. The passive properties parameters were estimated as in previous works (Benvenuti et al., 2006; Di Franco et al., 2016) by applying two step voltage pulses to −80 and −60 mV starting from a HP = −70 mV. Access resistance (R_a) was not compensated for monitoring membrane area. Series resistance was compensated up to 70 ± 90%. The area beneath the capacitive transient and the time constant of the transient's decay (τ) were used to calculate the cell linear capacitance (C_m) (see also Sartiani et al., 2007) and R_a from $\tau = R_a C_m$. The measurement of membrane resistance (R_m) were corrected for R_a and was calculated from the steady-state membrane current (I_m) using the relation: $R_m = (\Delta V - I_m R_a) / I_m$, where ΔV is the command voltage step amplitude. The ratio $1/R_m$, that is the membrane conductance G_m was used as an index of the resting cell permeability. C_m, was used as an index of the cell surface area assuming that membrane-specific capacitance is constant at 1 μF/cm^2. The membrane conductance G_m was normalized to cell linear capacitance (C_m) to allow comparison between different cells. The ratio G_m/C_m is then proposed as specific conductance.

RMP was recorded by switching to the current clamp mode of the 200 B amplifier. Experiments were performed at 22 °C.

2.4. Statistics

The statistical analysis of the results was attained by pClamp9 (Axon Instruments). To evaluate if RMP, passive membrane properties and I_{Ca} were significantly affected by neurotrophins respect to the control, data were statistically analyzed by means of Student's *t*-test. More than two groups were compared using ANOVA. When ANOVA indicated significant differences, the Newman-Keuls post-test for multiple comparisons between groups was performed. Experimental results are indicated as mean ± SEM. *P* value ≤0.05 was considered significant (confidence limits used are the 95%) unless otherwise specified. We assumed normally distributed samples.

3. Results

3.1. Effects of growth factors on n-HSP cells resting membrane potential and membrane passive properties

The analysis of resting membrane potential, RMP, achieved in current clamp mode showed that n-HSP had a mean value of −59.6 ± 3.53 mV in control condition (Fig. 1A, Ctr). Acute addition of BDNF or FGF2 (50 ng/ml) directly injected in the recording chamber caused appreciable effects on the cell membrane, appearing within 5 min of application. Both neurotrophins caused a transient membrane depolarization (−47.1 ± 4.0 and 49.8 ± 5.1 mV, see respectively Fig. 1Aa, BDNF (5′) and Fig. 1Ab, FGF2 (5′)) in respect to control values.

Then, to test the ability of the neurotrophins to facilitate the neuronal differentiation, n-HSP cells were pretreated with BDNF or FGF2 (50 ng/ml) before electrophysiological analysis. In line with our previous study (Sarchielli et al., 2014), we chronically treated n-HSP cells with BDNF or FGF2 for 24 h and this resulted in a significant membrane hyperpolarization (−67.6 ± 4.52 and −71.6 ± 7.5 mV, respectively) in respect to control values. Still in agreement with Sarchielli et al. (2014), we also performed experiments with neurotrophins receptor inhibitors: k252a (K) for BDNF and PD173074 (P) for FGF2. The 24-h pretreatment with BDNF and its receptor inhibitor K or with FGF2 and its receptor inhibitor P, induced a statistically significant membrane depolarization (−37.0 ± 6.93 and −45.5 ± 4.7 mV respectively), reaching voltages even more positive than control. However, we did not observe statistically significant differences between BDNF and FGF2 treatment (Fig. 1Aa and Ab, respectively). Prolonged treatment with neurotrophins (48 h) did not cause further alterations in RMP, which was not statistically different to control, as shown in Fig. 1Aa for BDNF treatment.

Successively, by switching to the voltage clamp mode of our device, we estimated the membrane passive properties. We first evaluated the cell capacitance C_m that is considered an index of cell surface (Fig. 1B). In a first set of experiments, BDNF or FGF2 were acutely added to the recording bath solution and electrophysiological measurements were made within 5 min from application. We observed that both BDNF and FGF2 caused a significant increase in cell capacitance (27.1 ± 2.8 and 25.0 ± 3.5 pF), respect to control (19.4 ± 2.9 pF), suggesting a rapid cell surface enlargement. Moreover, they induced an increase in G_m (3.5 ± 0.3 and 4.3 ± 0.4 nS respect to control, 2.9 ± 0.3 nS), and a decrease of specific conductance G_m/C_m (0.13 ± 0.03 and 0.17 ± 0.03 nS/pF respect to control, 0.19 ± 0.03 nS/pF) (Fig. 1C and D).

When the neurotrophins were chronically added in culture medium for 24 h they induced, respect to control, a statistically significant increase of C_m parameter (25.5 ± 1.6 pF in BDNF and 29.51 ± 4.8 in FGF2) suggesting a further cell surface enlargement. Once again, we observed that the pretreatment with the growth factors and their specific receptor inhibitors caused a consistent decrease in C_m (15.3 ± 1.7 and 16.0 ± 3.10 pF, respectively) respect to the growth factor alone and respect to control (Fig. 1 B). Finally, the membrane conductance (G_m) that is an index of resting cell membrane permeability (3.7 ± 0.21 nS in control) was significantly decreased by BDNF (2.6 ± 0.48 nS) and FGF2 treatment (2.6 ± 0.6 nS). The pretreatment with these growth factors and their receptor inhibitors definitely increased its value respect to control resulting 3.9 ± 0.3 and 4.4 ± 0.5 nS, respectively *vs.* 3.7 ± 0.21 nS (Fig. 1C). Similarly, the specific conductance (G_m/C_m) was also modified; being 0.1 ± 0.01 and 0.09 ± 0.01 nS/pF in BDNF and FGF2 respect to control (0.19 ± 0.02 nS/pF). The pretreatment with

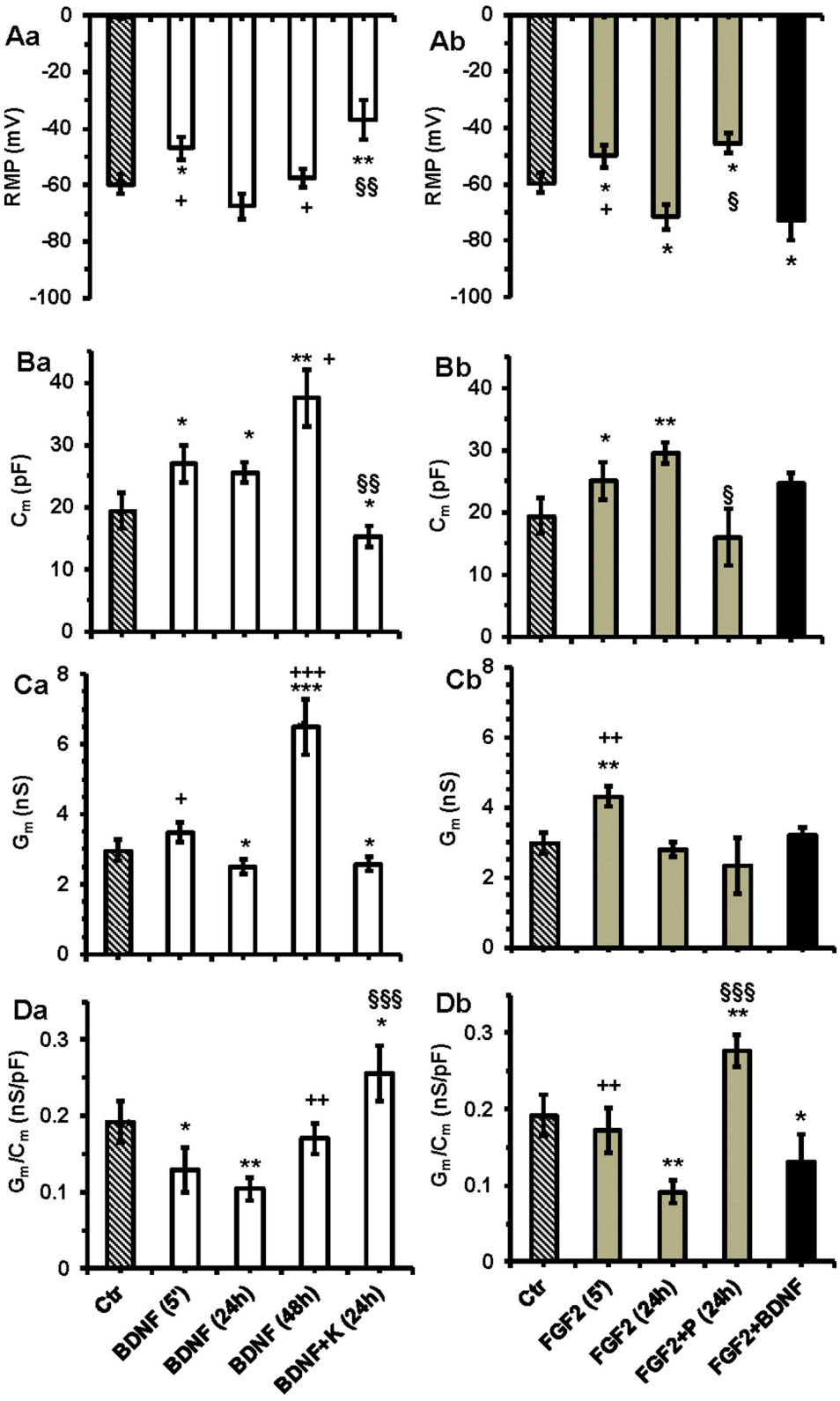

Fig. 1. Effects of BDNF and FGF2 on n-HSP cells RMP and resting membrane properties. Effects of growth factors as a function of time and of the presence of their receptor inhibitors, on RMP (A), C_m (B), G_m (C) and G_m/C_m (D). Ctr, untreated cells (dashed line bars) are the same in panels a and b. BDNF (white bars, panels a), FGF2 (grey bars, panels b) and FGF2 + BDNF (black bars, panels b). Acute treatment for any growth factor is indicated in the graphs as (5′). Chronical treatments with neurotrophins are indicated as BDNF (24 h), BDNF (48 h) and FGF2 (24 h). n-HSP cells in culture for 24 h with BDNF pretreated with its receptor inhibitor k252a (BDNF + K) or with FGF2 pretreated with its receptor inhibitor PD173074 (FGF2 + P); n-HSP cells in culture for 24 h with FGF2 and BDNF (FGF2 + BDNF). *, ** and *** indicate $P < 0.05$, $P < 0.01$ and $P < 0.001$ *vs* Ctr; $^{+}$, $^{++}$ and $^{+++}$ indicate $P < 0.05$, $P < 0.01$ and $P < 0.001$ *vs* 24 h treatment; §,§§ and §§§ indicate $P < 0.05$, $P < 0.01$ and $P < 0.001$ for BDNF or FGF2 plus their receptor inhibitor (BDNF + K and FGF2 + P) *vs* BDNF or FGF2 alone. Analyzed cells: $n = 42$ for Ctr; $n = 24$ for BDNF (24 h); $n = 30$ for FGF2 (24 h); $n = 8$ for acute and for 48 h-treatment; $n = 8$ for FGF2 + BDNF (24 h). Data are mean ± SEM.

neurotrophins and their receptor inhibitors gave 0.25 ± 0.03 and 0.27 ± 0.03 nS/pF, respectively (Fig. 1D).

To find out a possible synergistic effect we also investigated the combination of FGF2 + BDNF at the same time point. The results obtained are depicted as black bars in Fig. 1 (panels b). The RMP resulted significantly hyperpolarized respect to control, but not statistically different to values obtained with FGF2 treatment alone (Fig. 1Ab). The cell capacitance showed values similar to those obtained with BDNF alone (Fig. 1Ba and Bb), whereas G_m was slightly higher than those due to individual growth factors (Fig. 1Ca and Cb). Finally, G_m/C_m values showed a not statistically significant increase respect to individual growth factors (Fig. 1Da and Db).

Again, to determine if the neuronal response to neurotrophins changed as function of time, the same passive properties were measured also on n-HSP cells treated for 48 h. We observed a further net increase in C_m and G_m values, but the G_m/C_m values resulted not statistically different to control. As an example, we have reported the results obtained with BDNF in Fig. 1Ba, Ca and Da.

3.2. Ca^{2+} current type occurring in n-HSP cells

We then investigated the voltage-dependent Ca^{2+} currents, known to play a key role in neuronal functioning and neurotransmission. Ca^{2+} currents were first recorded in voltage clamp mode from n-HSP cells cultured in control condition for 24 h. Cells plated on the coverslip were placed in the recording chamber filled with the Na^+- and K^+-free solution (namely a TEA-Ca^{2+} bath solution) to record only Ca^{2+} currents.

Typical Ca^{2+} current traces were evoked from HP of −80 mV by depolarizing steps from −70 to 50 mV applied in 10 mV increments (Fig. 2Aa). As a confirmation, Cd^{2+} (100 μM) added in the bath solution blocked such currents (not shown, n = 7). We observed that inward currents were activated starting from −60 mV as transient currents (Fig. 2Ab). This low voltage of activation and the typical transient time course suggested the occurrence of the LVA T-type Ca^{2+} current in our preparation. Starting from −40 mV, this current superimposed on a slow activating and inactivating current that reached the maximal value with the 10 mV step, indicating also the presence of HVA current type. The mean total Ca^{2+} current density was 37.1 ± 4.3 pA/pF (n = 42) (Fig. 2B, filled circles). The plots of the total current peak amplitude *vs.* membrane potential show a shoulder at about −20 mV, suggesting the presence of several components (Fig. 2B, filled circles). To investigate in depth the different types of HVA Ca^{2+} currents involved, we made a pharmacological dissection by sequentially applying nifedipine (3 μM), ω-Ctx-GVIA (500 nM), and ω-Aga-IVA (200 nM) on the same n-HPS cell, to block L-, N-, and P/Q-type channels, respectively. Typical current traces elicited by a depolarizing pulse to 10 mV in control and after the adding of the Ca^{2+} channels blockers are depicted as an example in Fig. 2C. At this pulse potential in fact, all HVA currents types (L, N, P/Q and R) are about maximally activated and can be better discriminated by the use of specific blockers. The residual current observed in presence of the three specific blockers mentioned above was the result of LVA T-type plus the R-type Ca^{2+} currents. The single R-type Ca^{2+}-current component was estimated by blocking the T-type one by Ni^{2+} (Fig. 2Cb). Finally, the presence of T-type currents was confirmed after subtracting the traces recorded in the presence of Ni^{2+} (Fig. 2Cb), or evoked at HP = −40 mV, from the total Ca^{2+} currents. The complete representative families of the current traces obtained after pharmacological dissection are shown in Fig. 3. The 80% of the analyzed cells showed all the types of Ca^{2+} currents, whereas the 10% did not show the P/Q-type and in another 10% both the P/Q- and R-types were absent or hardly discernable from noise.

HVA Ca^{2+} currents were further characterized by studying their activation kinetics, measured as the maximal current elicited by the 10-mV step. The N-, R- and P/Q-type currents activated with time constants of 8.0 ± 0.6, 9.6 ± 0.8 and 6.5 ± 0.6 ms for N-, R- and P/Q-type, respectively. The L-type Ca^{2+} currents activated with a slower kinetics, having a time constant of 21.9 ± 0.2 ms. With regard to inactivation phase, the R-type Ca^{2+} currents could be fitted by an exponential function having a rather fast time constant of 80 ± 7 ms; in contrast, L-type currents inactivate following two rather slow exponentials (τ_1 = 360 ± 45 and τ_2 = 750 ± 82 ms), whereas P/Q and N type currents inactivate very slowly (about 1080–1100 ms). Finally, the LVA fast transient T-type currents elicited at −30 mV, activate and inactivate with time constant of 2.0 ± 0.2 and 4.5 ± 0.4 ms, respectively.

The *I/V* plots related to each single component isolated by pharmacological means are depicted in Fig. 4. The LVA T-type maximal current was elicited by the −20 mV-voltage pulse (Table 1). In contrast, the maximal peak amplitude of all the HVA currents was obtained with the 10-mV step, but each component showed different voltage thresholds of activation: P/Q- and R-type currents activated at about −30 mV whereas L- and N-types had a lower threshold of activation, being −50 and −40 mV, respectively (Fig. 4).

The *I/V* relationship of all the Ca^{2+} current types can be fitted by a single Boltzmann function, with half-maximal activation potentials around −5 mV for N-, P/Q and R-type and −2.0 ± 0.6 for L-type (see Tables 2–3). The HVA Ca^{2+} current type with the lowest voltage threshold of activation was the L-type, but V_a and the voltage eliciting the maximal Ca^{2+} current (V_p) were shifted to more positive potential (Tables 2–3). This nifedipine-sensitive L-type Ca^{2+} current was the main current type observed in these cells, with a maximal mean density of 24.1 ± 2.4 pA/pF. The other Ca^{2+} current types showed a mean density for ω-CgTx-GVIA-sensitive N-type Ca^{2+} current of 11.3 ± 1.1 pA/pF, for R-type of 5.5 ± 0.8 pA/pF, for ω-Aga-IVA-sensitive P/Q-type currents of 1.3 ± 0.5 pA/pF and for T-type 4.9 ± 0.7 pA/pF (Fig. 5A, Ctr).

3.3. Effects of growth factors on Ca^{2+} currents

The aim of the present study was to determine whether BDNF, known to regulate neuronal cell migration, and FGF2, could modulate voltage-dependent calcium currents in HSP cells. Accordingly, the measurements described above were repeated using n-HSP cells treated with BDNF (n = 24) or FGF2 (n = 30) for 24 h. Both BDNF and FGF2 treatment caused a reduction of the total Ca^{2+} current amplitude (Fig. 2B). In contrast, the treatment in the presence of their specific receptor inhibitor (BDNF + K and FGF2 + P) gave results similar to those obtained in control condition (Fig. 2B). However, to evaluate whether these neurotrophins had effect on a definite type of Ca^{2+} current, we applied the same procedure described above for analyzing L-, N-, P/Q, R- and T-type Ca^{2+} currents separately. Our results showed that the kinetics (V_a and k_a Boltzmann parameters) of such channels was not significantly affected. Nonetheless, L- and T-type current specific maximal size ($I_{Ca,max}/C_m$) and conductance (G_m/C_m) were reduced by a similar amount (about the 50%) both by BDNF and FGF2 (Figs. 4 and 5; Tables 1 and 2).

In contrast, $I_{Ca,max}/C_m$ and G_m/C_m of N-type Ca^{2+} currents were enhanced, but FGF2 caused a stronger effect than BDNF. Finally, these treatments did not significantly affect the Boltzmann parameters of P/Q and R type Ca^{2+} currents (Figs. 4 and 5; Table 3). The combination of both neurotrophins together at the same time point, did not give significant differences respect to individual growth factors (data not shown).

For completeness, also in this case n-HSP cells were cultured in the presence of the neurotrophins and their related receptor inhibitor for 24 h. In this condition, the specific maximal current size and conductance were reverted to values not statistically different respect to control (Figs. 4 and 5; Tables 1–3).

To test if this neuronal response to neurotrophins varied as function of time, we made further experiments at different time points (see Fig. 5).

Acute treatment caused in both cases a reduction of L-type Ca^{2+} current that was more evident under BDNF. N-type Ca^{2+} current resulted

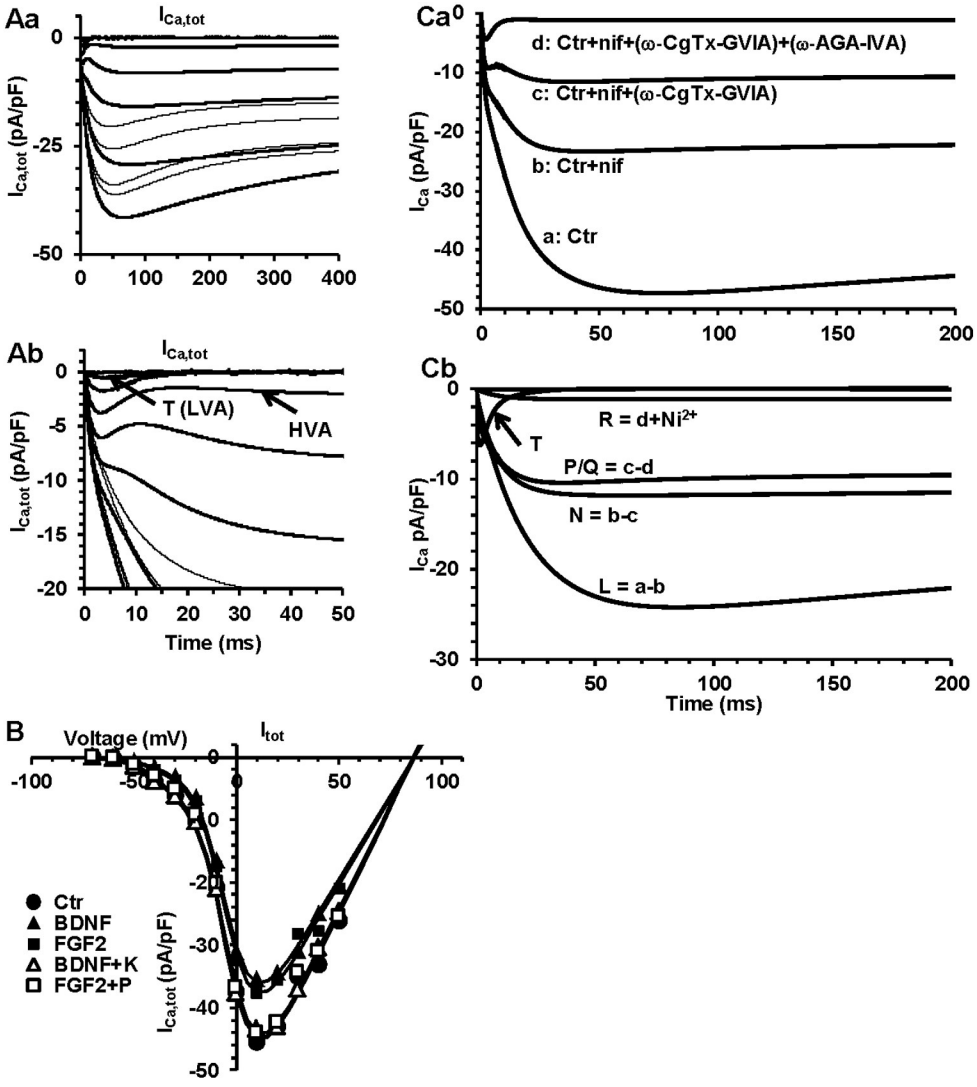

Fig. 2. Voltage-dependent Ca^{2+} current and pharmacological dissection of the different components in n-HSP cells. Aa) Typical family of total Ca^{2+} current traces elicited from HP = −80 mV in control condition; voltage steps ranging −70 to 50 mV in 10-mV increments. Ab) Same traces as in Aa, showed with a different ordinate scale to better observe the occurrence of LVA and HVA Ca^{2+} currents. B) Current *vs* voltage relationship (*I/V* plots) of the maximum specific total Ca^{2+} currents in control (filled circles) and after the treatment with BDNF or FGF2 (24 h) alone (filled triangles and squares, respectively) and together with their specific receptor inhibitor BDNF + K or FGF2 + P (open triangles and squares, respectively). Data are the mean values of $n = 42$ (Ctr), 24 (BDNF), 30 (FGF2), 16 (BDNF + K) and 14 (FGF2 + P) different cells. Ca) Pharmacological dissection of different Ca^{2+} currents: for clarity, only a typical Ca^{2+} current trace evoked by the voltage pulse at 10 mV (HP = −80 mV) is depicted for any treatment. Control condition (a trace: Ctr) and after the application of the specific L-type Ca^{2+} channel blocker nifedipine (3 μM) (b trace: Ctr + Nif). In sequence, ω-conotoxin-GVIA (v-CgTx-GVIA) (500 nM) was added to block N-type current (c trace) and ω-agatoxin-IVA (v-Aga-IVA) (200 nM) to block P/Q-type current (d trace); the residual current is the transient T- type Ca^{2+} current superimposed on R-type Ca^{2+} current (d trace). Cb) Typical single Ca^{2+} current-components obtained by subtracting trace b from a (L-type current = a–b), c from b (N type current = b–c) and d from c (P/Q type current = c–d). R-type component is obtained after application of Ni^{2+} (200 μM) to block T-type Ca^{2+} current; T-type Ca^{2+} current was obtained by subtracting R-type Ca^{2+} current trace depicted in Ca from R trace in Cb.

significantly enhanced by FGF2, but not by BDNF. The other high and low-voltage activated components were not significantly altered by the neurotrophins directly added to the bath solution.

In order to add a later time point to our analysis, we recorded the effect on Ca^{2+} currents from n-HSP cells treated for 48 h. We found that T- and L-type Ca^{2+} currents were not significantly altered respect to 24 h, whereas the N-type was the only one further increased by this longer treatment. Again, no other HVA currents were affected by the growth factors respect to control. Results obtained with BDNF for each type of Ca^{2+} current, are depicted as histograms in Fig. 5.

3.4. Effects of dopaminergic agonists on n-HSP cells

To test another important indicator of the differentiation state, we also aimed to investigate the effect of dopaminergic agonists on membrane properties and Ca^{2+} currents. Since a previous study of our research group (Sarchielli et al., 2014) showed that our n-HSP cells expressed D1 and D2 receptors mRNA, we tested the effect of SKF82958 or quinpirole selective for D1- and D2-dopamine receptors, acutely applied to the bath solution.

We consistently found that each dopaminergic agonist induced a slight membrane hyperpolarization of 3.1 ± 0.2 for quinpirole and 2.3 ± 0.2 mV for SKF82958. An example of representative tracings elicited in current clamp during application of the quinpirole and SKF is reported in Fig. 6A and B. Both dopaminergic agonists affected the membrane passive properties: they induced a decrease of cell capacitance that was more evident for SKF. In contrast, the resting and specific conductance were definitely enhanced, especially by quinpirole, but reduced by SKF respect to control (Fig. 6D–F).

We also tested the ability of dopaminergic agonists to modulate the calcium channel function in n-HSP cells. We could clearly observe that

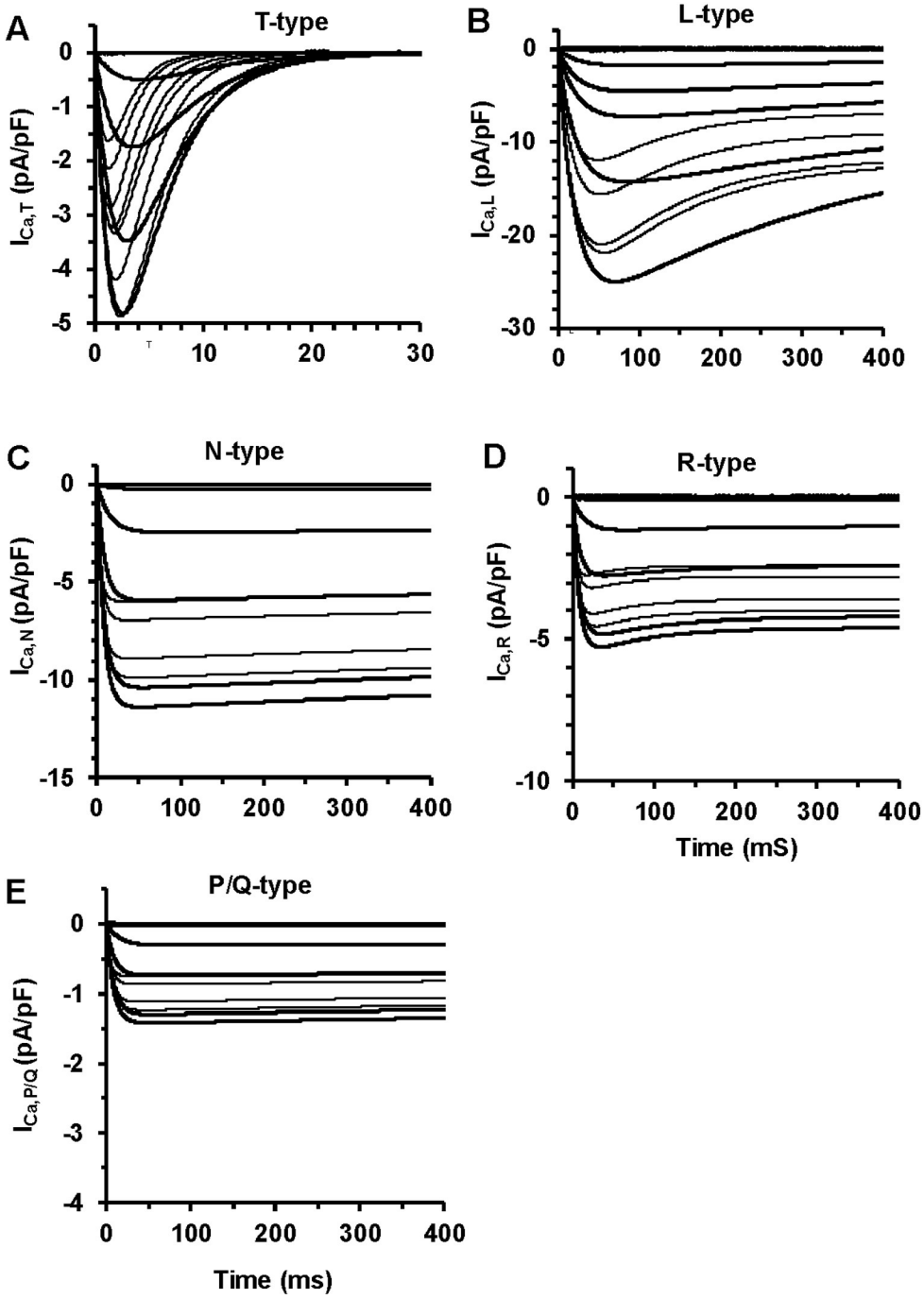

Fig. 3. Time course of different types of Ca^{2+} current in a single n-HSP cell. Typical families of current traces evoked in control conditions; voltage steps ranged from −70 to 50 mV in 10-mV increments (HP = −80 mV). A–E) Each family of traces related to a single component is obtained by the mathematical subtraction according to the method as in Fig. 2.

they were able to significantly decrease L- as well as N-type calcium current amplitude without altering the R-, P/Q- and T-type (Fig. 6G).

4. Discussion

In the present study, we examined human neuronal cells from striatal precursors isolated from human fetuses obtained as described in detail in Sarchielli et al. (2014). As showed by the Authors, HSP cells expressed D1 and D2 receptors mRNA, and since the expression of dopamine receptors is a good indicator of differentiation state, we tested the effects of dopaminergic agonists on membrane properties and their ability to modulate Ca^{2+} currents. Although from a functional point of view our cells are quite immature precursors, as suggested by the absence of action potentials firing, n-HSP were already capable to respond to D1 and D2 agonists. In fact, the treatment with their agonists hyperpolarized the resting membrane potential, changed the passive membrane properties and decreased L-, N- and P/Q-type Ca^{2+} current amplitude.

Moreover, as recently published by Sarchielli et al. (2014), our cells express neurotrophins, such as FGF2 and BDNF, along with the cognate receptors FGFR1 and TrkB, respectively. Particularly, FGF2 can be accumulated in extracellular matrix and may be internalized (Presta et al., 2005), whereas BDNF binds to TrkB (Reichardt, 2006; Zhang et al., 2012). This regulates the expression and activity of functionally important proteins such as ion channels and neurotransmitter receptors, and consequently regulates synaptic strength and plasticity (Vicario-Abejón

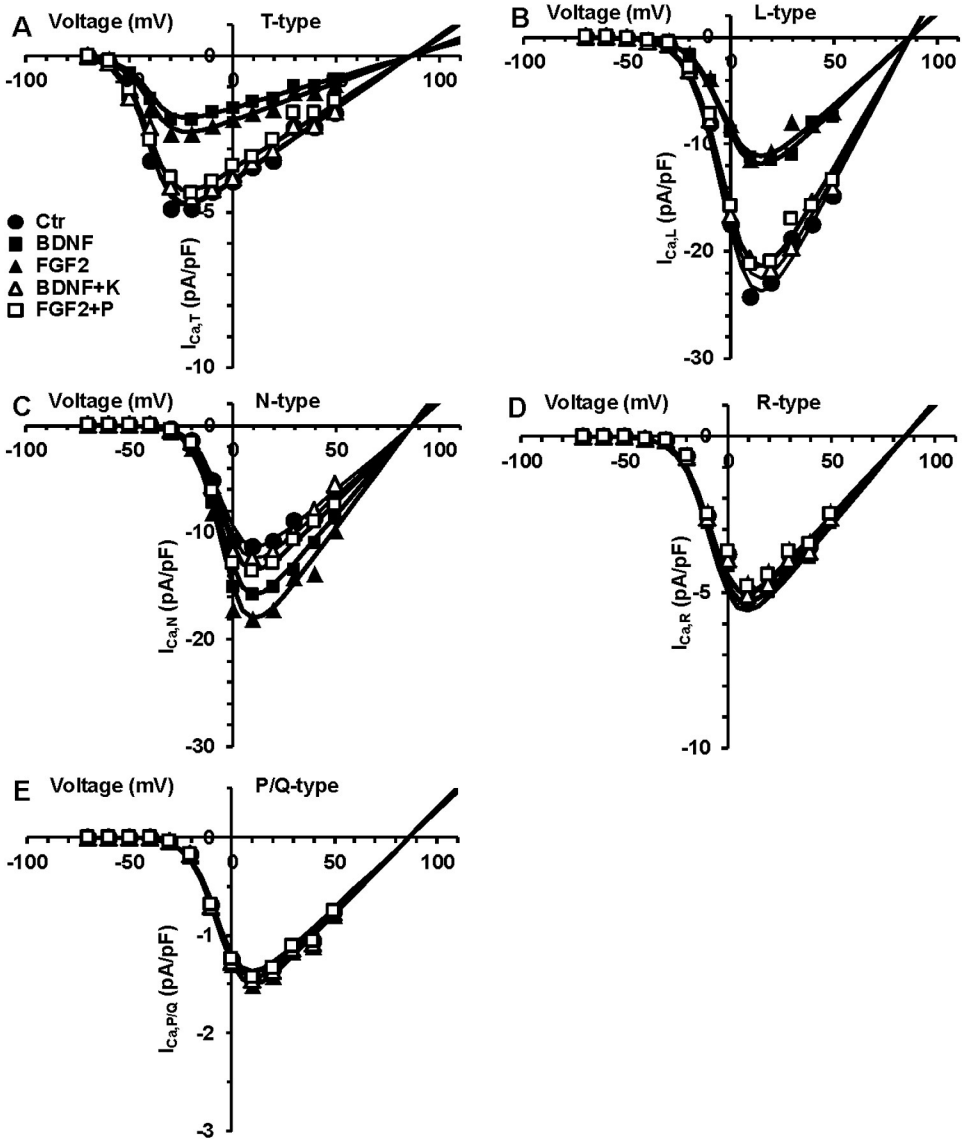

Fig. 4. Effects of BDNF or FGF2 treatment, alone and in the presence of their receptor inhibitors, on the different types of Ca^{2+} currents evoked in n-HSP cells. A–E) Current *vs* voltage relationship (*I*/*V* plots) of the single Ca^{2+}-current types from experiments as in Fig. 3, in the different culture conditions: in control (filled circles) and after the 24-h treatment with BDNF or FGF2 alone (filled squares and triangles, respectively) and together with their specific receptor inhibitor BDNF + K or FGF2 + P (open triangles and squares, respectively). The best fit to the experimental data points for any Ca^{2+} current type is obtained by a single Boltzmann function. Boltzmann parameters are listed in Tables 1–3. Data are the mean values of $n = 42$ (Ctr), 24 (BDNF), 30 (FGF2), 16 (BDNF + K) and 14 (FGF2 + P) different cells.

et al., 2002; Chao, 2003). When exogenously administered for 24 h, both neurotrophins have shown the ability to induce migration, survival and neuritogenesis of HSP cells (Sarchielli et al., 2014) and stronger modifications of the membrane properties (present study), thus suggesting a maturation of the main component of HSP cell population towards a more typical neuronal phenotype.

After having elucidated the biophysical properties of our cells, in this research we mainly focused on Ca^{2+} currents modulation by the neurotrophins, since Ca^{2+} channels are considered good markers of the cell fate and neuronal differentiation. In fact, the Ca^{2+} ions entry is known to control a variety of crucial functions in neurons, including the cell excitability, the neurotransmitter release, somato-dendritic retrograde release and other intracellular events. Ca^{2+} ions can enter the cell through a variety of channels and between these, the voltage-operated Ca^{2+} channels are typically grouped into a number of classes based on their voltage-dependence and pharmacological properties. Accordingly, different types of Ca^{2+} currents can be described in neurons: the low-voltage-activated (LVA) T-type currents and the high voltage-activated (HVA) currents; these latter can be distinguished into L-, N-, P/Q- and R-type. These voltage-operated Ca^{2+} channels are crucial for different biological events and are regulated by various signalling pathways, which has profound functional consequences (Wu et al., 2002). Notably, the expression of the type of Ca^{2+} channels depends on the stage of differentiation of the type of neuron considered and of the transcripts expressed. Accordingly, the kind of Ca^{2+} current detected is a good indicator of the cell fate. In fact, Ca^{2+} currents are very small in amplitude or completely absent in neuronal stem cells (Moe et al., 2005). In contrast, they appear in neuronal precursors with a prevalent L-type Ca^{2+} current (D'Ascenzo et al., 2006).

It is well known that in neurons, Ca^{2+} influx *via* presynaptic Ca^{2+} channels is an obligatory step for neurotransmission that gives rise to a complex cascade of events in the synaptic junction. However, the presynaptic terminals do not necessarily express the same combination of Ca^{2+} channel types, even when terminals emanate from the same axon. The different types of Ca^{2+}-channels are located in different cell sites (Hell et al., 1993; Westenbroek et al., 1990) and are prevalently involved in different functions (Joux et al., 2001; Reid et al., 2003; Catterall and Goswami et al., 2012). For example, the L-type and T-type Ca^{2+}

Table 1
Boltzmann parameters of T-type I_{Ca} activation curve in n-HSP cells cultured for 24 h in control solution (Ctr), in the presence of BDNF or FGF2 alone or with their specific inhibitor added (K and P, respectively).

Parameters	Ctr	BDNF	FGF2	BDNF + K	FGF2 + P
$I_{Ca,T}$					
$I_{Ca,max}/C_m$ (pA/pF)	4.9 ± 0.6	2.0 ± 0.4**	2.5 ± 0.3**,§	4.8 ± 0.8	3.9 ± 0.8
G_m/C_m (pS/pF)	47.1 ± 4	18.9 ± 3**	23.6 ± 4**,§	46.2 ± 5	37.3 ± 5
V_p (mV)	−25.2 ± 2	−26.5 ± 2	−25.9 ± 2	−25.4 ± 3	−25.3 ± 3
V_a (mV)	−40.0 ± 4	−41.2 ± 2	−41.6 ± 1	−40.6 ± 1	−40.9 ± 2
k_a (mV)	6.5 ± 0.4	6.3 ± 0.5	6.7 ± 0.4	6.6 ± 0.6	6.6 ± 0.5
V_{rev} (mV)	86.0 ± 7	88.4 ± 9	88.3 ± 8	87.3 ± 8	86.2 ± 9

Both neurotrophins increase the maximum peak of the specific current size, $I_{Ca,max}/C_m$, and the related maximal G_m/C_m. Data are mean ± S.E.M. Data from Ctr: $n = 42$; BDNF $n = 24$, FGF2 $n = 30$; BDNF + K $n = 16$ and FGF2 + P $n = 14$.
** $P < 0.01$ treated cells *vs* control.
§ $P < 0.05$ FGF2 *vs* BDNF.

channels are not normally involved in excitatory transmitter release; the N-type channels might be selectively expressed at recently formed terminals, or in a 'reserve' pool of terminals held in an immature state, whereas P/Q-type channels might dominate at fully mature and active terminals (Momiyama, 2003).

Since the aim of this research was to evaluate the effect of two neurotrophins on our cell model, it must be considered that any growth factor may selectively affect the different types of Ca^{2+} channels and the sensitivity may vary among the different kinds of neurons (Yang and Tsien, 1993; Colston et al., 1998; Bouron et al., 2006). Moreover, the final effects may depend on how neurotrophins are delivered (Ji et al., 2010). Thus, the temporal aspect in cell signalling may also have implications for the therapeutic drug design and since our cells express TrkB (Sarchielli et al., 2014) this feature can be relevant also in the present study. In fact, experiments achieved with acute application of BDNF showed different effects on passive properties and different modulation of Ca^{2+} currents respect to chronical treatment. This can be considered in good in agreement with Ji et al. (2010), that observed that the two modes of BDNF delivery also caused very different morphological changes in cultured hippocampal neurons and further supports a critical role of the kinetic of TrkB activation for cell signalling and functions.

It is known that the activity of voltage-operated ion channels can be finely regulated by neurotransmitters, growth/trophic factors and hormones (Bean, 1989; Boland and Bean, 1993; Wu et al., 2002). In the present study, we found that n-HSP cells cultured in control condition showed all the LVA and HVA Ca^{2+} current types. Among these, the L-type was the prevalent one whereas N-, R-, T- and P/Q types showed a progressively minor amplitude. Notably, we observed that the chronical treatment with BDNF and FGF2 neurotrophins definitely affected the voltage-dependent Ca^{2+} current occurrence, likely ascribable to a sustained TrkB activation. In fact, both BDNF and FGF2 reduced T- and L-type specific current-amplitude and conductance, while enhanced that of N-type Ca^{2+} channels. In contrast, P/Q- and R-type Ca^{2+} current were not appreciably affected by the treatments. Parallel changes of the maximal amplitude and conductance were determined by the neurotrophins with no effects on V_a or k_a Boltzmann parameters. Hence, we suggest that chronical treatment with FGF2 and BDNF does not substantially affect the ion channels kinetics but can be effective in changing the functional expression of different Ca^{2+} channels on the plasma membrane, in agreement with the idea that sustained activation of neurotrophin receptor and signal transduction events may alter gene expression (Ji et al., 2010). However, we observed that these two growth factors induced somehow different effects, since BDNF caused a more marked reduction of L- and T-type Ca^{2+} currents than FGF2 did. A similar outcome has already been described for BDNF in embryonic cortical neurons of the mouse, where BDNF was shown to down-regulate Ca^{2+} currents, acting as potent modulator of the electrical properties of early post-mitotic neurons, thus exerting a neuroprotective action (Bouron et al., 2006). In contrast, we found that FGF2 was more effective in enhancing N-type current respect to BDNF, suggesting a major efficiency of FGF2 in promoting the acquisition of the channels mostly involved in the neuronal excitatory transmitter release.

In this regard, it is to note that FGF2 is an important promoter of proliferation in neuronal progenitor cells, but in neural crest cells for instance, FGF2 treatment alone does not lead to cell expansion, rather requiring the presence of a neurotrophin such as BDNF, nerve growth factor or neurotrophin-3 (Sieber-Blum, 1998). As well, in neural stem cells of the rat, the combination of growth factors has been reported to have an additive effect on neural differentiation (Choi et al., 2008). However, no synergistic morphoregulatory effects of neurotrophins or

Table 2
Boltzmann parameters of L- and N-type Ca^{2+} activation curves in n-HSP cells cultured for 24 h in control solution (Ctr), in the presence of BDNF or FGF2 alone or with their specific K and P inhibitor added.

Parameters	Ctr	BDNF	FGF2	BDNF + K	FGF2 + P
$I_{Ca,L}$					
$I_{Ca,max}/C_m$ (pA/pF)	24.0 ± 2	10.1 ± 1**	9.7 ± 0.8**	13.2 ± 2	21.6 ± 3
G_m/C_m (pS/pF)	368.6 ± 23	131.5 ± 11**	123.6 ± 12**	249.8 ± 29	236.6 ± 30
V_p (mV)	15.2 ± 2	15.5 ± 2	15.9 ± 2	15.4 ± 2	15.3 ± 2
V_a (mV)	−2.0 ± 0.6	−2.2 ± 0.5	−2.4 ± 0.6	−1.8 ± 0.8	−1.9 ± 0.9
k_a (mV)	8.0 ± 0.4	7 ± 0.6	7.7 ± 0.5	7.9 ± 0.6	7.8 ± 0.6
$I_{Ca,N}$					
$I_{Ca,max}/C_m$ (pA/pF)	11.3 ± 0.8	15.8 ± 1**	18.1 ± 0.9**,§	12.4 ± 1	13.6 ± 1
G_m/C_m (pS/pF)	162.0 ± 19	226.8 ± 20**	259.2 ± 22**,§	178.2 ± 18	194.4 ± 21
V_p (mV)	10.2 ± 1	10.5 ± 2	11.1 ± 2	10.8 ± 2	10.3 ± 2
V_a (mV)	−4.5 ± 0.4	−4.2 ± 0.4	−4.1 ± 0.5	−4.6 ± 1	−4.9 ± 1
k_a (mV)	6.5 ± 0.4	6.3 ± 0.5	6.2 ± 0.4	6.6 ± 0.6	6.7 ± 0.5
V_{rev} (mV)	84.0 ± 7	85.8 ± 9	84.1 ± 8	86.1 ± 9	86.6 ± 9

Neurotrophins reduce the maximum peak current size, $I_{Ca,max}/C_m$ and the related maximal G_m/C_m of L-type channels; in contrast, they increase those of N-type Ca^{2+} current. Number of cells as in Table 1.
** $P < 0.01$ treated cells *vs* control
§ $P < 0.05$ FGF2 *vs* BDNF.

Table 3
Boltzmann parameters of P/Q- and *R*-type Ca^{2+} activation curve in n-HSP cells cultured for 24 h in control solution (Ctr), in the presence of BDNF or FGF2 alone or with their specific K and P inhibitor added.

Parameters	Ctr	BDNF	FGF2	BDNF + K	FGF2 + P
$I_{Ca,P/Q}$					
$I_{Ca,max}/C_m$ (pA/pF)	1.3 ± 0.2	1.4 ± 0.3	1.4 ± 0.4	1.4 ± 0.4	1.3 ± 0.4
G_m/C_m (pS/pF)	19.7 ± 2	21.4 ± 2	20.5 ± 2	19.8 ± 2	19.6 ± 3
V_p (mV)	10.3 ± 1	10.1 ± 2	9.9 ± 2	10.4 ± 2	10.3 ± 2
V_a (mV)	−5.8 ± 0.6	−5.9 ± 0.5	−6.2 ± 0.6	−5.7 ± 0.8	−5.8 ± 0.9
k_a (mV)	6.7 ± 0.4	6.3 ± 0.5	6.7 ± 0.4	6.5 ± 0.6	6.7 ± 0.6
V_{rev} (mV)	87.0 ± 7	86.8 ± 9	88.4 ± 8	86.1 ± 9	86.5 ± 10
$I_{Ca,R}$					
$I_{Ca,max}/C_m$ (pA/pF)	5.5 ± 0.6	5.6 ± 1	5.5 ± 0.8	6.2 ± 1	5.3 ± 3
G_m/C_m (pS/pF)	63.6 ± 6	64.5 ± 6	65.6 ± 5	64.1 ± 29	63.6 ± 30
V_p (mV)	10.2 ± 2	12.5 ± 2	9.9 ± 2	11.4 ± 2	10.3 ± 2
V_a (mV)	−7.1 ± 0.6	−7.2 ± 0.5	−6.6 ± 0.6	6.8 ± 0.8	6.9 ± 0.9
k_a (mV)	6.9 ± 0.4	6.3 ± 0.5	6.7 ± 0.4	6.7 ± 0.6	6.8 ± 0.6
V_{rev} (mV)	88.0 ± 7	88.8 ± 9	88.2 ± 8	88.1 ± 9	89.2 ± 10

Boltzmann parameters of cells cultured with growth factors with or without the related receptor inhibitor are similar to the control. Number of cells as in Table 1.

growth factors were detected on dentate gyrus neurons from postnatal rat (Patel and McNamara, 1995). Accordingly, when we treated n-HSP cells with the combination of BDNF and FGF2 we did not actually observe a clear synergistic effect, since only the membrane conductance values resulted slightly higher than those due to individual growth factors. No significant alterations were observed in Ca^{2+}-currents expression/functionality. Since growth factors are supposed to act in concert in different cell lineages and in several aspects of neural crest cell development, including survival, proliferation, and differentiation, the underlying mechanisms that involve growth-factor-induced dependence of the cells on other factors definitely deserves further investigation in a dedicated study.

Therefore, by an electrophysiological point of view, BDNF and FGF2 have clear effects on n-HSP cells. Since T-type calcium channel family (CaV_T) is present throughout the striatum as well as in the accumbens nucleus (Talley et al., 1999), the T-type Ca^{2+} current may represent a potential pacemaker current of this region of the central nervous system (Moody and Bosma, 2005) and thus may play a role in spontaneous firing activity. Accordingly, any reduction of this kind of current can reduce eventual pacemaker activity of HSP cells, with functional consequences *in vivo*. Moreover, the HVA Ca^{2+} channels that are characterized by a relatively slow activation and incomplete inactivation can be activated by the LVA transient T-type Ca^{2+} current. This in turn can activate *N*-, *R*- and P/Q-types, with their higher voltage threshold and fast activation kinetics, possibly suggesting a greater contribution of early Ca^{2+} entry during neuronal activity. It should also be remarkable to determine in depth the relative involvement of these different current types to Ca^{2+} ions entry during electrical activity of n-HSP cells, as well as to identify the various Ca^{2+}-dependent processes triggered by the activation of each specific channel. Particularly, in this study, the BDNF and FGF2 induced the enhancement of N-type Ca^{2+} current and this may strongly suggest that HSP cells have attained a physiologically more differentiated phenotype. In fact, in neurons, the activation of the voltage-gated N-type Ca^{2+} channel plays a significant role in

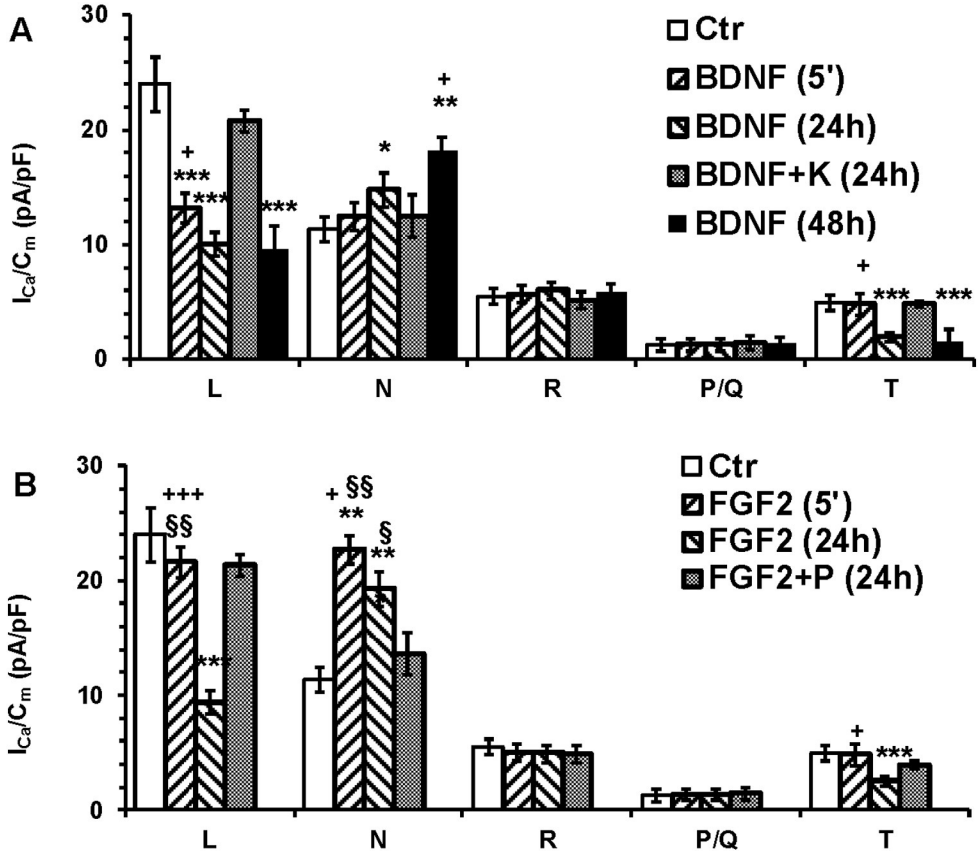

Fig. 5. Effect of BDNF and FGF2 as a function of time on L-, *N*-, *R*-, P/Q- and T-type Ca^{2+} currents. The effects of BDNF (A) and FGF2 (B) on L-, N- and T-type maximal peak currents vary with time. Different times of exposure are displayed in the legends next to each panel. Peak current evoked by the voltage pulse at 10 mV (HP = −80 mV) for L-, N-, R- and P/Q-type and at −20 mV for T-type current. *, ** and *** indicate $P < 0.05$, $P < 0.01$ and $P < 0.001$ *vs* Ctr; $^{+}$ and $^{+++}$ indicate $P < 0.05$ and $P < 0.001$ *vs* 24 h treatment; § and §§ indicate $P < 0.05$ and $P < 0.01$ *vs* the same current under BDNF. Data are from the same cells of Fig. 4. Values are mean ± SEM. Peak currents are normalized for cell capacitance and reported in pA/pF.

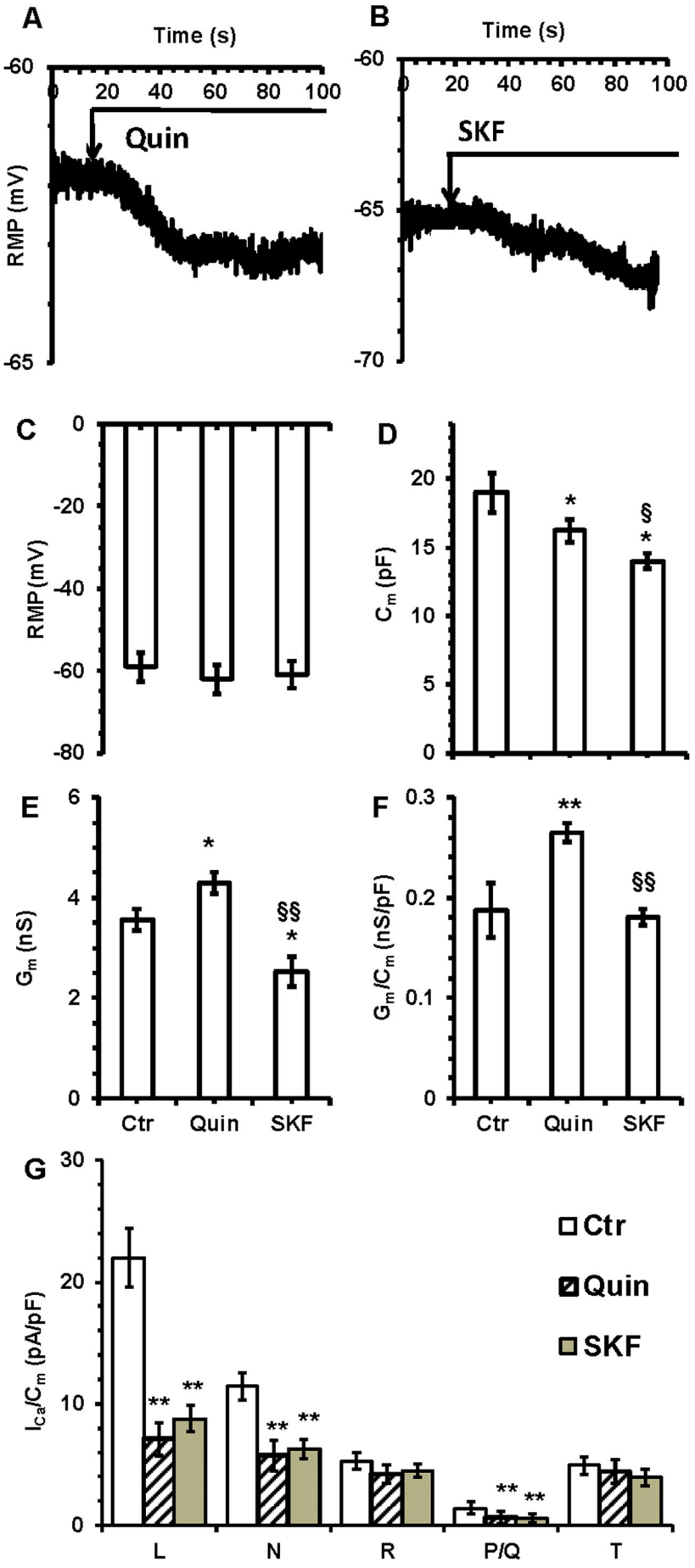
A
Time (s)
-60
0 20 40 60 80 100
Quin
RMP (mV)
-65
B
Time (s)
-60
0 20 40 60 80 100
SKF
-65
-70
C
0
-20
-40
-60
-80
RMP (mV)
D
20
15
10
5
0
C_m (pF)
*
§
*
E
6
4
2
0
G_m (nS)
*
§§
*
Ctr
Quin
SKF
F
0.3
0.2
0.1
0
G_m/C_m (nS/pF)
**
§§
Ctr
Quin
SKF
G
30
20
10
0
I_{Ca}/C_m (pA/pF)
**
**
**
**
**
**
L
N
R
P/Q
T
Ctr
Quin
SKF

multiple cellular functions such as the neurotransmitter release, the regulation of gene expression, the dendritic development and synaptic plasticity (Toselli et al., 2005).

To further support this clue, we observed that both neurotrophins affected also the resting membrane properties, suggesting the growth of the surface area, the RMP hyperpolarization, the reduction of the resting total and specific membrane conductance, that is usually observed upon differentiation (Moe et al., 2005). The decrease in membrane conductance might have been caused by the decrease of membrane leak non-specific current and/or to a lower expression of additional ionic channels (Picken Bahrey and Moody, 2003). Therefore, this last finding may indicate the achievement of an improved control of depolarizing ionic influx such as leakage and/or voltage independent currents and this may have relevance *in vivo* in assessing the correct excitability.

These results are in good agreement with our previous demonstration that both neurotrophins stimulate neuritogenesis in HSP cells (Sarchielli et al., 2014). In addition, we point out a pronounced effect of external addition of BDNF and FGF2 on voltage-activated Ca^{2+} currents that typically occur in untreated HSP cells. Particularly, FGF2 is known to bind to surface membrane receptors, can be accumulated in extracellular matrix and may be internalized (Presta et al., 2005). Thus, the treatment with FGF2 and BDNF in the presence of their specific receptor inhibitors can blunt not only the action of the growth factors externally added to the bath solution, but also the effect of those growth factors present on the membrane surface and internalized inside the cells. Accordingly, we observed that the effect due to the growth factor inhibitors was greater than expected, thus further supporting the hypothesis about the role of an endogenous production of both BDNF and FGF2 by HSP cells, as previously suggested (Sarchielli et al., 2014).

5. Conclusions

In conclusion, the treatment with BDNF and FGF2 is able to induce specific modifications in the biophysical membrane properties of n-HSP cells and differently modulate the various Ca^{2+} currents suggesting that these neurotrophins are important factors in promoting HSP neuronal cell maturation. Moreover, the hypothesized endogenous production of both factors by HSP cells could be important for the regenerative potential of fetal striatal grafts in HD patients. However, future studies addressing the effects of FGF2 and BDNF on electrophysiological properties not only in wild type but also in HD neurons could be of help to assess the therapeutic value of these growth factors or advance our understanding of the degenerative nature of HD.

Acknowledgements

The Authors would like to thank Dr. Erica Sarchielli (Department of Experimental and Clinical Medicine, University of Florence) for her help in cell culture experiments.

This research has been funded by University of Florence, Grant no 58513PAS1314 to RS.

References

Ambrosini, S., Sarchielli, E., Comeglio, P., Porfirio, B., Gallina, P., Morelli, A., Vannelli, G.B., 2015. Fibroblast growth factor and endothelin-1 receptors mediate the response of human striatal precursor cells to hypoxia. Neuroscience 289, 123–133.

Armstrong, R.J., Watts, C., Svendsen, C.N., Dunnett, S.B., Rosser, A.E., 2000. Survival, neuronal differentiation, and fiber outgrowth of propagated human neural precursor grafts in an animal model of Huntington's disease. Cell Transplant. 9, 55–64.

Bachoud-Lévi, A.C., Gaura, V., Brugières, P., Lefaucheur, J.P., Boissé, M.F., Maison, P., Baudic, S., Ribeiro, M.J., Bourdet, C., Remy, P., Cesaro, P., Hantraye, P., Peschanski, M., 2006. Effect of foetal neural transplants in patients with Huntington's disease 6 years after surgery: along-term follow-up study. Lancet Neurol. 5, 303–309.

Bean, B.P., 1989. Neurotransmitter inhibition of neuronal calcium currents by changes in channel voltage dependence. Nature 340, 153–156.

Benvenuti, S., Saccardi, R., Luciani, P., Urbani, S., Deledda, C., Cellai, I., Francini, F., Squecco, R., Rosati, F., Danza, G., Gelmini, S., Greeve, I., Rossi, M., Maggi, R., Serio, M., Peri, A., 2006. Neuronal differentiation of human mesenchymal stem cells: changes in the expression of the Alzheimer's disease-related gene seladin-1. Exp. Cell Res. 312, 2592–2604.

Boland, L.M., Bean, B.P., 1993. Modulation of N-type calcium channels in bullfrog sympathetic neurons by luteinizing hormone-releasing hormone: kinetics and voltage dependence. J. Neurosci. 12, 516–533.

Bouron, A., Boisseau, S., De Waard, M., Peris, L., 2006. Differential down-regulation of voltage-gated calcium channel currents by glutamate and BDNF in embryonic cortical neurons. Eur. J. Neurosci. 24, 699–708.

Catterall, W.A., Swanson, T.M., 2015. Structural basis for pharmacology of voltage-gated sodium and calcium channels. Mol. Pharmacol. 88, 141–150.

Chao, M.V., 2003. Neurotrophins and their receptors: a convergent point for many signaling pathways. Nat. Rev. Neurosci. 4, 299–309.

Choi, K.C., Yoo, D.S., Cho, K.S., Huh, P.W., Kim, D.S., Park, C.K., 2008. Effect of single growth factor and growth factor combinations on differentiation of neural stem cells. J. Korean Neurosurg. Soc. 44, 375–381.

Cicchetti, F., Saporta, S., Hauser, R.A., Parent, M., Saint-Pierre, M., Sanberg, P.R., Li, X.J., Parker, J.R., Chu, Y., Mufson, E.J., Kordower, J.H., Freeman, T.B., 2009. Neural transplants in patients with Huntington's disease undergo disease-like neuronal degeneration. Proc. Natl. Acad. Sci. U. S. A. 106, 12,483–12,488.

Cohen-Cory, S., Kidane, A.H., Shirkey, N.J., Marshak, S., 2010. Brain-derived neurotrophic factor and the development of structural neuronal connectivity. Dev. Neurobiol. 70, 271–288.

Colston, J.T., Valdes, J.J., Chambers, J.P., 1998. Ca^{2+} α_1-subunit transcripts are differentially expressed in rat pheochromocytoma (PC12) cells following nerve growth factor treatment. Int. J. Dev. Neurosci. 16, 379–389.

D'Ascenzo, M., Piacentini, R., Casalbore, P., Budoni, M., Pallini, R., Azzena, G.B., Grassi, C., 2006. Role of L-type Ca^{2+} channels in neural stem/progenitor cell differentiation. Eur. J. Neurosci. 23, 935–944.

Di Franco, A., Guasti, D., Squecco, R., Mazzanti, B., Rossi, F., Idrizaj, E., Gallego-Escuredo, J.M., Villarroya, F., Bani, D., Forti, G., Barbara Vannelli, G., Luconi, M., 2016. Searching for classical brown fat in humans: development of a novel human fetal brown stem cell model. Stem Cells http://dx.doi.org/10.1002/stem.2336 (Epub ahead of print).

Gallina, P., Paganini, M., Lombardini, L., Saccardi, R., Marini, M., De Cristofaro, M.T., Pinzani, P., Salvianti, F., Crescioli, C., Di Rita, A., Bucciantini, S., Mechi, C., Sarchielli, E., Moretti, M., Piacentini, S., Gritti, G., Bosi, A., Sorbi, S., Orlandini, G., Vannelli, G.B., Di Lorenzo, N., 2008. Development of human striatal anlagen after transplantation in a patient with Huntington's disease. Exp. Neurol. 213, 241–244.

Gallina, P., Paganini, M., Lombardini, L., Mascalchi, M., Porfirio, B., Gadda, D., Marini, M., Pinzani, P., Salvianti, F., Crescioli, C., Bucciantini, S., Mechi, C., Sarchielli, E., Romoli, A.M., Bertini, E., Urbani, S., Bartolozzi, B., De Cristofaro, M.T., Piacentini, S., Saccardi, R., Pupi, A., Vannelli, G.B., Di Lorenzo, N., 2010. Human striatal neuroblasts develop and build a striatal-like structure into the brain of Huntington's disease patients after transplantation. Exp. Neurol. 222, 30–41.

Goswami, S.P., Bucurenciu, I., Jonas, P., 2012. Miniature IPSCs in hippocampal granule cells are triggered by voltage-gated Ca^{2+} channels via microdomain coupling. J. Neurosci. 32, 14,294–14,304.

Grothe, C., Timmer, M., 2007. The physiological and pharmacological role of basic fibroblast growth factor in the dopaminergic nigrostriatal system. Brain Res. Rev. 54, 80–91.

Hell, J.W., Westenbroek, R.E., Warner, C., Ahlijanian, M.K., Prystay, W., Gilbert, M.M., Snutch, T.P., Catterall, W.A., 1993. Identification and differential subcellular localization of the neuronal class C and class D L-type calcium channel α1 subunits. J. Cell Biol. 123, 949–962.

Heubach, J.F., Graf, E.M., Leutheuser, J., Bock, M., Balana, B., Zahanich, I., Christ, T., Boxberger, S., Wettwer, E., Ravens, U., 2004. Electrophysiological properties of human mesenchymal stem cells. J. Physiol. 554, 659–672.

Ji, Y., Lu, Y., Yang, F., Shen, W., Tang, T.T., Feng, L., Duan, S., Lu, B., 2010. Acute and gradual increases in BDNF concentration elicit distinct signaling and functions in neurons. Nat. Neurosci. 13, 302–309.

Joux, N., Chevaleyre, V., Alonso, G., Boissin-Agasse, L., Moos, F.C., Desarménien, M.G., Hussy, N.N., 2001. High voltage-activated Ca^{2+} currents in rat supraoptic neurones: biophysical properties and expression of the various channel α1 subunits. J. Neuroendocrinol. 13, 638–649.

Li, G.R., Sun, H., Deng, X., Lau, C.P., 2005. Characterization of ionic currents in human mesenchymal stem cells from bone marrow. Stem Cells 23, 371–382.

Moe, M.C., Varghese, M., Danilov, A.I., Westerlund, U., Ramm-Pettersen, J., Brundin, L., Svensson, M., Berg-Johnsen, J., Langmoen, I.A., 2005. Multipotent progenitor cells from the adult human brain: neurophysiological differentiation to mature neurons. Brain 128, 2189–2199.

Momiyama, T., 2003. Parallel decrease in ω-conotoxin*n*-sensitive transmission and dopamine-induced inhibition at the striatal synapse of developing rats. J. Physiol. 546, 483–490.

Moody, W.J., Bosma, M.M., 2005. Ion channel development, spontaneous activity, and activity-dependent development in nerve and muscle cells. Physiol. Rev. 85, 883–941.

Fig. 6. Effect of dopaminergic agonists on RMP, passive properties and Ca^{2+} currents in *n*-HSP cells. Representative current traces elicited in current clamp as showed in Fig. 3, during acute application of the D2-agonist quinpirole (Quin) 10 μM (A) or D1-agonist SKF, 10 μM (B). Effect of quinpirole application ($n = 8$) and SKF ($n = 7$) on RMP (C), on C_m (D), G_m (E) and G_m/C_m (F). G) Peak current evoked by the voltage pulse at 10 mV (HP = −80 mV) for *L*-, *N*-, *R*- and P/Q-type and at −20 mV for T-type current. Values are mean ± SEM. Peak currents are normalized for cell capacitance and reported in pA/pF. $^{*}P < 0.05$ and $^{**}P < 0.01$ *vs* control; $^{§}P < 0.05$ and $^{§§}P < 0.01$ SKF *vs* Quin.

Novak, M.J., Tabrizi, S.J., 2010. Huntington's disease. BMJ 340, c3109.
Obeso, J.A., Rodríguez-Oroz, M.C., Benitez-Temino, B., Blesa, F.J., Guridi, J., Marin, C., Rodriguez, M., 2008. Functional organization of the basal ganglia: therapeutic implications for Parkinson's disease. Mov. Disord. 23, S548–S559.
Onorati, M., Castiglioni, V., Biasci, D., Cesana, E., Menon, R., Vuono, R., Talpo, F., Goya, R.L., Lyons, P.A., Bulfamante, G.P., Muzio, L., Martino, G., Toselli, M., Farina, C., Barker, R.A., Biella, G., Cattaneo, E., 2014. Molecular and functional definition of the developing human striatum. Nat. Neurosci. 17, 1804–1815.
Paganini, M., Biggeri, A., Romoli, A.M., Mechi, C., Ghelli, E., Berti, V., Pradella, S., Bucciantini, S., Catelan, D., Saccardi, R., Lombardini, L., Mascalchi, M., Massacesi, L., Porfirio, B., Di Lorenzo, N., Vannelli, G.B., Gallina, P., 2014. Fetal striatal grafting slows motor and cognitive decline of Huntington's disease. J. Neurol. Neurosurg. Psychiatry 85, 974–981.
Park, H., Poo, M.M., 2013. Neurotrophin regulation of neural circuit development and function. Nat. Rev. Neurosci. 14, 7–23.
Patel, M.N., McNamara, J.O., 1995. Selective enhancement of axonal branching of cultured dentate gyrus neurons by neurotrophic factors. Neuroscience 69, 763–770.
Peschanski, M., Cesaro, P., Hantraye, P., 1995. Rationale for intrastriatal grafting of striatal neuroblasts in patients with Huntington's disease. Neuroscience 68, 273–285.
Picken Bahrey, H.L., Moody, W.J., 2003. Early development of voltage-gated ion currents and firing properties in neurons of the mouse cerebral cortex. J. Neurophysiol. 89, 1761–1773.
Presta, M., Dell'Era, P., Mitola, S., Moroni, E., Ronca, R., Rusnati, M., 2005. Fibroblast growth factor/fibroblast growth factor receptor system in angiogenesis. Cytokine Growth Factor Rev. 16, 159–178.
Reichardt, L.F., 2006. Neurotrophin-regulated signalling pathways. Philos. Trans. R. Soc. Lond. Ser. B Biol. Sci. 361, 1545–1564.
Reid, C.A., Bekkers, J.M., Clements, J.D., 2003. Presynaptic Ca^{2+} channels: a functional patchwork. Trends Neurosci. 26, 683–687.
Reuter, I., Tai, Y.F., Pavese, N., Chaudhuri, K.R., Mason, S., Polkey, C.E., Clough, C., Brooks, D.J., Barker, R.A., Piccini, P., 2008. Long-term clinical and positron emission tomography outcome of fetal striatal transplantation in Huntington's disease. J. Neurol. Neurosurg. Psychiatry 79, 948–951.
Sah, D.W., Ray, J., Gage, F.H., 1997. Regulation of voltage- and ligand-gated currents in rat hippocampal progenitor cells in vitro. J. Neurobiol. 32, 95–110.
Sarchielli, E., Marini, M., Ambrosini, S., Peri, A., Mazzanti, B., Pinzani, P., Barletta, E., Ballerini, L., Paternostro, F., Paganini, M., Porfirio, B., Morelli, A., Gallina, P., Vannelli, G.B., 2014. Multifaceted roles of BDNF and FGF2 in human striatal primordium development. An in vitro study. Exp. Neurol. 257, 130–147.
Sartiani, L., Bettiol, E., Stillitano, F., Mugelli, A., Cerbai, E., Jaconi, M.E., 2007. Developmental changes in cardiomyocytes differentiated from human embryonic stem cells: a molecular and electrophysiological approach. Stem Cells 25, 1136–1144.
Sieber-Blum, M., 1998. Growth factor synergism and antagonism in early neural crest development. Biochem. Cell Biol. 76, 1039–1050.
Talley, E.M., Cribbs, L.L., Lee, J.-H., Daud, A., Perez-Reyes, E., Bayliss, D.A., 1999. Differential distribution of three members of a gene family encoding low voltage-activated (T-type) calcium channels. J. Neurosci. 19, 1895–1911.
Toselli, M., Biella, G., Taglietti, V., Cazzaniga, E., Parenti, M., 2005. Caveolin-1 expression and membrane cholesterol content modulate N-type calcium channel activity in NG108-15 cells. Biophys. J. 89, 2443–2457.
Tuszynski, M.H., 2007. Rebuilding the brain: resurgence of fetal grafting. Nat. Neurosci. 10, 1229–1230.
Vicario-Abejón, C., Owens, D., McKay, R., Segal, M., 2002. Role of neurotrophins in central synapse formation and stabilization. Nat. Rev. Neurosci. 3, 965–974.
Watmuff, B., Pouton, C.W., Haynes, J.M., 2012. In vitro maturation of dopaminergic neurons derived from mouse embryonic stem cells: implications for transplantation. PLoS One 7, e31999.
Westenbroek, R.E., Ahlijanian, M.K., Catterall, W.A., 1990. Clustering of L-type Ca^{2+} channels at the base of major dendrites in hippocampal pyramidal neurons. Nature 347, 281–284.
Westerlund, U., Moe, M.C., Varghese, M., Berg-Johnsen, J., Ohlsson, M., Langmoen, I.A., Svensson, M., 2003. Stem cells from the adult human brain develop into functional neurons in culture. Exp. Cell Res. 289, 378–383.
Wu, L., Bauer, C.S., Zhen, X.G., Xie, C., Yang, J., 2002. Dual regulation of voltage-gated calcium channels by PtdIns(4,5)P2. Nature 419, 947–952.
Yang, J., Tsien, R.W., 1993. Enhancement of N- and L-type calcium channel currents by protein kinase C in frog sympathetic neurons. Neuron 10, 127–136.
Zhang, F., Kang, Z., Li, W., Xiao, Z., Zhou, X., 2012. Roles of brain-derived neurotrophic factor/tropomyosin-related kinase B (BDNF/TrkB) signalling in Alzheimer's disease. J. Clin. Neurosci. 19, 946–949.
Zuccato, C., Valenza, M., Cattaneo, E., 2010. Molecular mechanisms and potential therapeutical targets in Huntington's disease. Physiol. Rev. 90, 905–981.